ELSEVIER

Journal of Power Sources 68 (1997) 674–679

JOURNAL OF POWER SOURCES

Observation of structure change due to discharge/charge process of V_2O_5 prepared by ozone oxidation method, using in situ X-ray diffraction technique

Yuichi Sato *, Tsuneyoshi Asada, Hideaki Tokugawa, Koichi Kobayakawa

Department of Applied Chemistry, Faculty of Engineering, Kanagawa University, Rokkakubashi, Kanagawa-ku, Yokohama 221, Japan

Accepted 13 November 1996

Abstract

The change in structure of vanadium pentoxide due to the discharge/charge process of V_2O_5 prepared by the ozone oxidation method (O_3–V_2O_5) was studied using an in situ X-ray diffraction technique. The diffraction peaks of (600), (020), (420) and (710) shifted to lower angles as Li^+ intercalation progressed until about $x=0.8$. Then they disappeared and a new broad peak appeared at 47°, which means that lattice extension and structure change occurred. When the O_3–V_2O_5 was discharged to $x=1.8$ and then charged, the XRD pattern recovered to almost its initial pattern. The change in the chemical diffusion coefficient (D) for O_3–V_2O_5 measured using the GIT and the AC techniques closely corresponded to the behavior observed using the in situ XRD technique, i.e. the change in diffusion coefficient levelled at about $x=0.8$, but after that the value of D decreased. The changes in the chemical diffusion coefficients of other types of V_2O_5 (orthorhombic, electrochemically prepared and amorphous V_2O_5) were also measured and their changes due to Li^+ intercalation are discussed. © 1997 Published by Elsevier Science S.A.

Keywords: Vanadium pentoxide; Crystal structure changes; Cycling behavior; Diffusion coefficient; Ozone oxidation method

1. Introduction

High energy density cathode active materials for rechargeable lithium batteries are being developed with great enthusiasm. Vanadium pentoxide is one of the most promising materials among the available candidates. Matsushita and Toshiba have commercialized coin-type batteries using orthorhombic V_2O_5 (o-V_2O_5). In addition to o-V_2O_5, many other types of non-crystalline V_2O_5-related compounds, including xerogel $V_2O_5 \cdot nH_2O$ [1,2], V_2O_5–P_2O_5 [3,4], aerogel V_2O_5 [5] and others have also been investigated as the possible cathode materials. We have already reported that electrochemically prepared V_2O_5 (e-V_2O_5) from a $VOSO_4$ solution [6] exhibited an intermediate crystal structure and displayed an electrochemical behavior between that of o-V_2O_5 and amorphous V_2O_5–P_2O_5 (a-V_2O_5–P_2O_5). V_2O_5 prepared by the ozone oxidation method (O_3–V_2O_5) is another new type of V_2O_5 that shows almost the same characteristics as e-V_2O_5 [7,8]. Recently, Hibino et al. [9] prepared a new type of V_2O_5(2D-V_2O_5) by the direct reaction of metallic vanadium with hydrogen peroxide and provided a structural model, showing that it exists in a form intermediate between the amorphous and crystalline stages [9,10]. The X-ray diffraction (XRD) patterns of e- and O_3–V_2O_5 were found to coincide with those of 2D-V_2O_5, the structure of these two compounds being almost similar [10]. We studied changes in the structure of a new type of V_2O_5(O_3–V_2O_5) with orthorhombic V_2O_5(o-V_2O_5) during discharge and charge using an in situ XRD technique; it is important to study changes in the structure in order to understand the limits of discharge capacity and cycleability. The changes in the chemical diffusion coefficients of Li^+ in four types of V_2O_5 (O_3-, e-, o-, and amorphous V_2O_5–P_2O_5 (a-V_2O_5–P_2O_5)) were also measured using GIT [11] and AC [12] techniques, since it is also important to infer those structural changes occurring as Li^+ intercalation progresses and to estimate the possibilities for high rate charge/discharge characteristics.

2. Experimental

e-V_2O_5 [6], O_3–V_2O_5 [7,8] and a-V_2O_5–P_2O_5 [13] with a nominal composition of 5 mol% P_2O_5 were prepared according to methods used in previous papers. The o-V_2O_5

* Corresponding author.

PII S0378-7753(96)02640-7

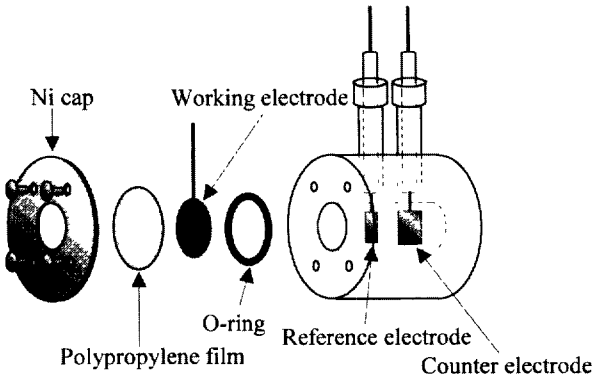

Fig. 1. Construction of the in situ XRD cell

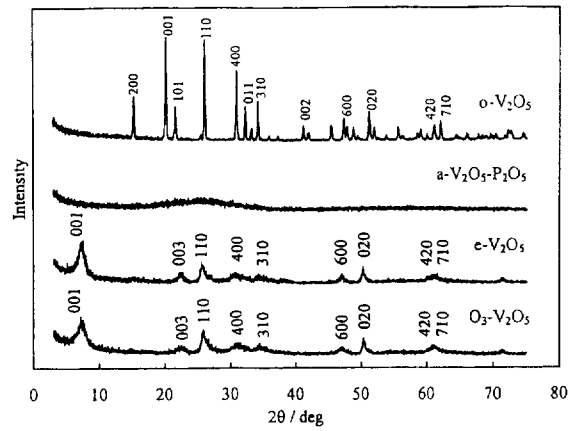

Fig. 2. XRD patterns of four types of V_2O_5.

was a reagent-grade commercial product (Woko Junyaku). A cathode for in situ XRD measurement was fabricated by mixing 82 wt.% O_3–V_2O_5 or o-V_2O_5, 14 wt.% conductive binder (acetylene black:polytetrafluoroethylene:surface active agent (66:33:1)) and 4 wt.% silicon or gold powder. The mixture was pressed onto a nickel mesh collector to make a 3.14 cm^2 tablet. Silicon and gold were used as the standard for the reflection angle. The cathode was placed in the electrolyte cell for in situ XRD measurement as shown in Fig. 1. XRD patterns were recorded with a Rigaku diffractometer (Rad-γA) for V_2O_5 powder and a Rigaku diffractometer (CN2013) for in situ measurement using monochromatic Cu Kα radiation. The V_2O_5 electrode was reduced by applying a 0.50 mA/cm^2 cathodic current for o-V_2O_5 and 0.32 mA/cm^2 for O_3–V_2O_5, and in situ XRD measurement was carried out at room temperature. In the case of the diffusion coefficient measurement, the cathode was fabricated by mixing 71 wt.% V_2O_5, 14 wt.% graphite and 15 wt.% conductive binder. The mixture was pressed onto a nickel mesh collector to make a 1.33 cm^2 tablet. For both the in situ XRD and the diffusion coefficient measurements were carried out in 1 M $LiClO_4$/propylene carbonate (PC) (Mitsubishi Chemical). The reference and counter electrodes were lithium foils. The diffusion coefficient (D) was measured by applying a -0.17 mA/cm^2 cathodic pulse current for 15 min corresponding to $x=0.025$ for GIT technique. Impedance was measured by applying 10 mV between 100 kHz and 1 MHz for the AC technique at 30 °C. Open-circuit voltages (OCV) as a function of composition were obtained by a constant current of -0.17 mA/cm^2 and equilibration on open circuit for 6 h.

3. Results and discussion

3.1. XRD measurement

In Fig. 2, the XRD patterns of four types of V_2O_5 are shown. Those for e-V_2O_5 and O_3–V_2O_5 show the same diffraction patterns, and coincide with that of V_2O_5 prepared by the reaction of metallic vanadium and hydrogen peroxide [9]. The structure of the e- and O_3–V_2O_5 seems to be intermediate between those of orthorhombic (o-V_2O_5) and a-V_2O_5–P_2O_5. It is noted that all reflection peaks of e- and O_3–V_2O_5 compounds coincide in the 2θ angle with the ($hk0$) reflection of o-V_2O_5 except for a strong peak at about 7.6° and a weak peak at 23.4°. The patterns for both e- and O_3–V_2O_5 compounds are characterized by a diffuse peak shape, rising rapidly and then continuously decreasing toward the high angle side. These features indicate that the compound has taken a random layer lattice structure, which consists of layers (a–b) arranged at equidistant and in parallel, but random in translation parallel to the layer and rotation about the normal c-axis [14]. In such cases, there will be a crystalline reflection of (001), a two-dimensional lattice reflection of (hk) and no general reflection of (hkl). Thus, the peaks at 7.6° and 23.4° may correspond to (001) and (003) reflection [10]. The lattice parameters of O_3–V_2O_5 are $a=11.6$ Å, $b=3.62$ Å, and $c=11.6$ Å, respectively. These values a and b are slightly greater than those for o-V_2O_5, while the value of c is much higher than that for o-V_2O_5 ($c=4.37$ Å) and is close to that known for the interlayer distance in the V_2O_5 xerogel containing water molecules. By thermogravimetric analysis, it was found that O_3–V_2O_5 contains about 0.5 mol% of water. Thus, a water layer is surmised to be present between two planer layers, which enlarges the value of c in O_3–V_2O_5 in comparison with o-V_2O_5. The XRD peaks at 7.6° due to (001) and at 23.4° due to (003) observed in air shifted to 9.9° and 31°, respectively, in a dry argon atmosphere or in an electrolyte solution. These results indicate that O_3–V_2O_5 is unstable in air, and absorbs water to change its structure. It is therefore important to study the changes in structure of O_3–V_2O_5 during the discharge process by in situ measurement without removing the cathode material. Before measuring the change in the structure of O_3–V_2O_5, the changes in o-V_2O_5 during the discharge process were studied by in situ measurement. The change in XRD patterns of o-V_2O_5 at various values of x are shown in Fig. 3. As Li^+ intercalated into o-

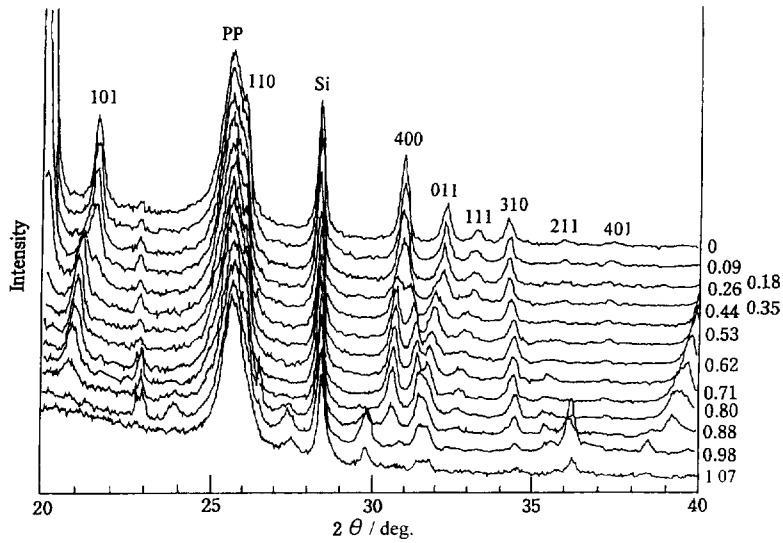

Fig. 3. In situ XRD patterns of o-V_2O_5 at various states of discharge.

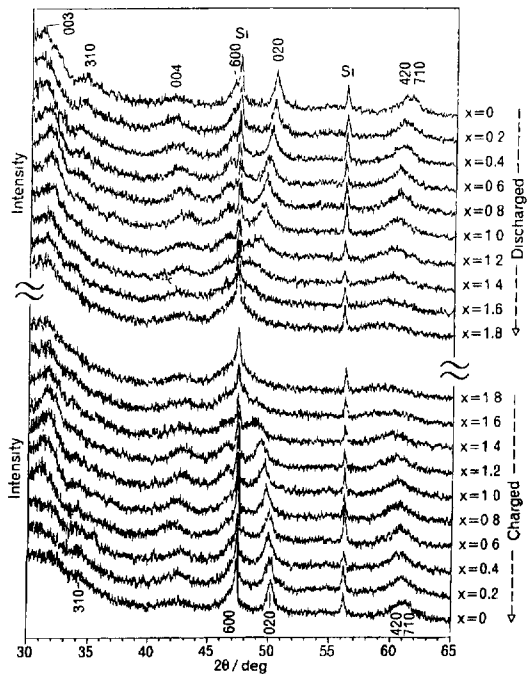

Fig. 4. In situ XRD patterns of O_3–V_2O_5 containing Si powder at various discharge/charge states.

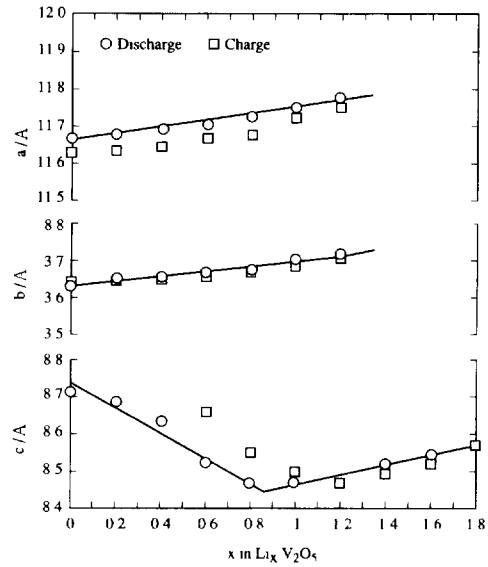

Fig. 5. Lattice parameters of O_3–V_2O_5 at various states of (○) discharge and (□) charge.

V_2O_5, the diffraction peaks of (011) and (101) shifted to lower angles, with the latter disappearing at about $x=0.8$. The peak at 31° split at $x=0.3$–0.4. At $x=0.8$–0.9, new diffraction peaks appeared at 24°, 27.5°, 30° and 36° suggesting that the crystal structure changed at these stages. These XRD pattern changes are consistent with those obtained by Cocciantelli et al. [15]. Namely, during the initial stage of the discharge, a rhombic-form phase appeared, which seems to change to ϵ-V_2O_5 at about $x=0.3$, and then to δ-V_2O_5 at about $x=0.8$–0.9.

Figs. 4 and 5 show the in situ XRD pattern changes of O_3–V_2O_5 for the discharging and charging processes, and the changes in lattice parameters obtained by these XRD patterns. The ($hk0$) reflection peaks shifted to lower angles and the reflection of (003) and (004) shifted to higher angles between $x=0$ and $x=0.8$, as Li^+ is intercalated (Fig. 4), indicating that lattice constants a and b increased while c decreased (Fig. 5). Starting at an $x\sim0.8$, the reflection of $l=0$ broadened and finally disappeared, while the reflection peaks of (003) and (004) did not disappear, but shifted to

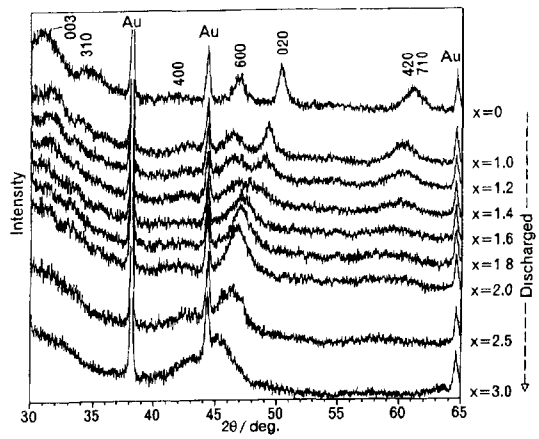

Fig. 6. In situ XRD patterns of O_3–V_2O_5 containing Au powder at various states of discharge.

lower angles, and lattice constant c started to increase. These behaviors closely corresponded with changes in diffusion constant for O_3–V_2O_5, as is discussed later. At about $x=0.8$, the initial structure is destroyed by Li^+ insertion and a new phase seems to appear, which may interfere with Li^+ diffusion. At $x \sim 1.4$, a new peak appears at 47° even though it is not that clear, since it is disturbed by the reflection of Si. After being changed from Si to Au as the standard for the reflection angle, the peak appeared more clearly, which may be due to a new structure (Fig. 6). However, the assignment of this peak at 47° is still unknown. During the charging process, the XRD patterns followed almost a reverse of the traces seen in Fig. 4. The structure of the O_3–V_2O_5 seems to hold for charge/discharge cycling between $x=0$ and $x=1.8$. Actually, the cycleability of O_3–V_2O_5 is better than that of o-V_2O_5 [8]. The value of c at $x=0$ is 8.7 Å as seen in Fig. 5 and is different from that (11.6 Å) obtained by the XRD patterns shown in Fig. 2. The former value is obtained for the dried state sample, and the water content present between two planer layers is probably small, while the latter value is obtained by the XRD spectrum measured in atmosphere and a water layer to be present between two planer layers, increasing the value of c.

3.2. Changes in diffusion coefficient

The open-circuit potential changes for four types of V_2O_5 needed for the calculation of the diffusion coefficients and the first discharge curves are shown in Fig. 7. When the cut-off voltage is 2.0 V, both the capacities of the e- and O_3–V_2O_5 compounds are 250–260 mAh/g for ten cycles. These capacities are higher than those for o-V_2O_5 and a-V_2O_5–P_2O_5. The potential change due to Li^+ intercalation is reasonable, as suggested from their cyclic voltammograms [8] i.e., those for the e- and O_3–V_2O_5 compounds are intermediate between o-V_2O_5 and a-V_2O_5–P_2O_5. The potentials of both the e- and O_3–V_2O_5 compounds decreased steadily with the slope changing at about $x=0.9$. Using the differences in potential between at $x=0$ and x, and other parameters, the chemical diffusion coefficients ($\tilde{D}$) for the four types of V_2O_5 were obtained (Fig. 8). In the case of o-V_2O_5, $\tilde{D}$ changed dramatically. This behavior coincided with information found in Ref. [16], and almost corresponding to the in situ XRD results mentioned above. The change in D is caused by a change in the crystal structure due to the insertion of Li^+. At first, $\tilde{D}$ decreased as Li^+ intercalation progressed, which might be due to interference by Li^+ already intercalated into

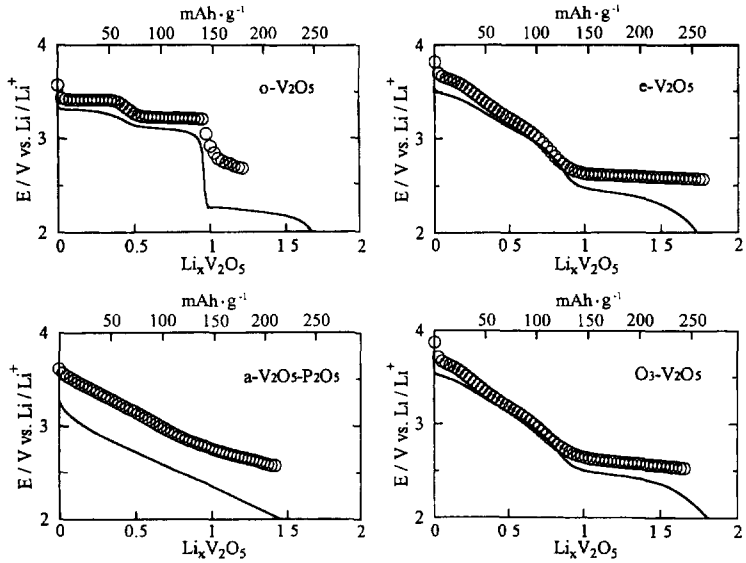

Fig. 7. Open-circuit potential changes and first discharge curves of four types of V_2O_5 at 30 °C.

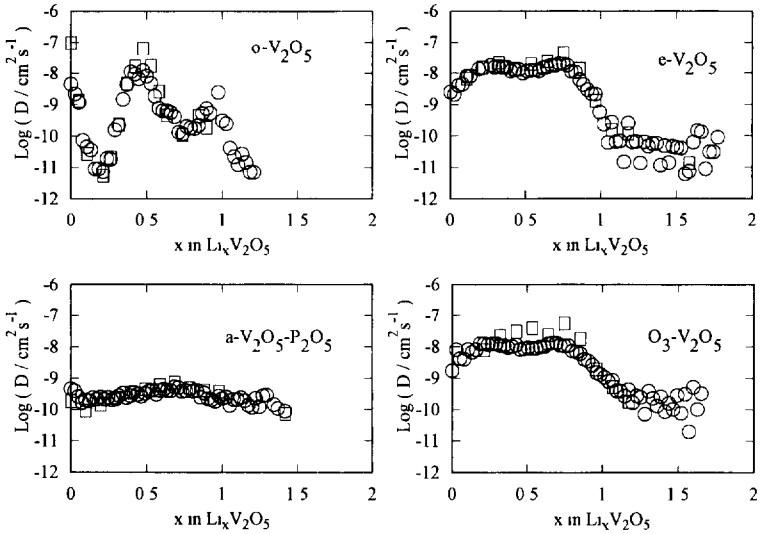

Fig. 8. Changes in chemical diffusion coefficient (D) of Li^+ vs. x at 30 °C in four types of V_2O_5: (○) GIT technique, and (□) AC technique.

the o-V_2O_5 layers. At $x \sim 0.2$, $\tilde{D}$ began to increase, which suggests that a structure change from α- to ϵ-V_2O_5 [15] occurred and that new space to accommodate Li^+ was formed. A similar structure change occurred at $x \sim 0.8$–0.9, when δ-V_2O_5 appeared [15] and the value of $\tilde{D}$ started to increase. With a-V_2O_5–P_2O_5, $\tilde{D}$ did not change as much as expected from the OCV curve, e.g. the a-V_2O_5–P_2O_5 structure is resistant to a structural destruction by Li^+ insertion. As expected from the OCV curves when x increases to ~0.8, the change in $\tilde{D}$ for both the e- and the O_3–V_2O_5 compounds was not as great as that for c-V_2O_5. Between $x = 0$ and $x = 0.8$, $\tilde{D}$ maintained a relatively high value in the order of 10^{-8} cm^2/s and then decreased to (10^{-10}–10^{-11}) cm^2/s. This suggests that a structural change occurs at about $x = 0.8$, which corresponded to the in situ XRD change (Figs. 4 and 5). From the four cases of the $\tilde{D}$ measurement, it was found that the GIT and the AC techniques provided almost the same values, therefore being considered as reliable techniques.

4. Conclusions

Structural changes due to the discharge process for V_2O_5 prepared from a $VOSO_4$ solution by ozone oxidation (O_3–V_2O_5) was not so that remarkable up to $x \sim 0.8$. Structural change occurred at $x > 0.8$. The change in the chemical diffusion constant of O_3–V_2O_5 due to Li^+ intercalation was consistant with the above change. Changes in the chemical diffusion coefficients of other types of V_2O_5, i.e. orthorhombic, electrochemically prepared and amorphous V_2O_5 were also measured and the change due to Li^+ intercalation was examined.

Acknowledgements

The authors express their thanks to Professor Isamu Uchida at Tohoku University for his kind teaching of the in situ XRD technique. The authors are grateful for the Grant-in-Aid for Scientific Research from the Japanese Ministry of Education (No. 05 650 834) and the Tokyo Ohka Foundation for the Promotion of Science and Technology.

References

[1] R. Baddour, J.P. Pereira-Ramos, R. Messina and J. Perichon, *J. Electroanal. Chem., 314* (1989) 81.
[2] T. Miura, S. Kunishiro, Y. Muranushi and T. Kishi, *Denki Kagaku, 57* (1989) 393.
[3] T. Pagnier, M. Fouletier and J.L. Souquet, *Solid State Ionics, 9/10* (1989) 649.
[4] Y. Sakurai and J. Yamaki, *J. Electrochem. Soc., 135* (1988) 791.
[5] D B. Le, S. Passerini, A.L. Tipton, B.B. Owens and W.H. Smyrl, *J Electrochem. Soc., 142* (1995) L102
[6] Y. Sato, T. Nomura, H. Tanaka and K. Kobayakawa, *J. Electrochem. Soc., 138* (1991) L37.
[7] Y. Sato, N. Matsueda, H. Tokugawa and K Kobayakawa, *Chem. Lett.*, (1993) 901
[8] Y. Sato, N. Matsueda, H. Tokugawa and K Kobayakawa, in B.M. Barnett, E. Dowgiallo, G. Halpert, Y. Matsuda and Z-I. Takehara (eds.), *Proc. Symp. New Sealed Rechargeable Batteries and Supercapacitors*, The Electrochemical Society Softbound Proc Series, Proc. Vol. 93-23, Pennington, NJ, USA, 1993, p 423.
[9] M. Hibino, M. Ugaji, A Kishimoto and T Kudo, *Solid State Ionics, 79* (1995) 239.
[10] M Ugaji, M. Hibino and T. Kudo, *J. Electrochem. Soc., 142* (1995) 3664

[11] W. Weppner and R A Huggins, *J. Electrochem. Soc.*, *124* (1977) 1569.
[12] C. Ho, I.D. Raistric and R.A Huggins, *J Electrochem. Soc.*, *127* (1980) 343
[13] Y. Sato, T. Nomura, H. Tanaka and K. Kobayakawa, in K M Abraham and M Saromon (eds), *Proc. Symp. Primary and Secondary Batteries*, The Electrochem. Soc. Softbound Proc. Series, Proc Vol 91-3, Pennington, NJ, USA, 1991, p. 335.
[14] B.E. Warren, *Phys Rev.*, *59* (1941) 693.
[15] J.M Cocciantelli, J.P Doumerc, M. Pouchard, M. Brussely and J. Labat, *J. Power Sources*, *34* (1991) 103.
[16] J. Farcy and R Messina, *J. Electrochem. Soc.*, *137* (1990) 1337.